

CEBAF Program Advisory Committee Six (PAC6) Proposal Cover Sheet

This proposal must be received by close of business on April 5, 1993 at:

CEBAF
User Liaison Office
12000 Jefferson Avenue
Newport News, VA 23606

Proposal Title

A measurement of the Fifth Structure Function via
Quasielastic ^{12}C , $^{16}\text{O}(\vec{e}, e'p)$

Contact Person

Name: Woo young Kim
Institution: University of Illinois
Address: Room 26-555, MIT
Address: Laboratory for Nuclear Science
City, State ZIP/Country: Cambridge, MA 02139
Phone: 617 253 4095 FAX: 617 258 5440
E-Mail → BITnet: Wooyoung@mit.hs Internet: Wooyoung@mit.hs.mit.edu

If this proposal is based on a previously submitted proposal or letter-of-intent, give the number, title and date:

CEBAF Use Only

Receipt Date: 4/5/93 Log Number Assigned: PR 93-042

By: sp

CEBAF Proposal for PAC6 June, 1993:

**A Measurement of the Fifth Structure Function via
Quasielastic ^{12}C , $^{16}\text{O}(\vec{e}, e'p)$**

R. Alarcon, J. R. Comfort, J. Gørgen, D. Martinez
Arizona State University

D. J. Abbott, L. S. Cardman, R. D. Carlini, D. J. Mack,
J. H. Mitchell, S. A. Wood*
Physics Division, CEBAF

O. K. Baker
*Physics Department, Hampton University,
and Physics Division, CEBAF*

M. K. Brussel, S. M. Dolfini, W. Kim*, J. B. Mandeville,
R. Laszewski, C. N. Papanicolas*, S. E. Williamson*
University of Illinois

J. R. Calarco, D. J. DeAngelis
University of New Hampshire

S. Boffi, C. Giusti, F. D. Pacati, M. Radici
Universita' di Pavia

* co-spokesman

Abstract

Using the polarized electron beam and the out-of-plane capability of the SOS in Hall C, we propose to measure the electron helicity asymmetry, A_e , for ^{12}C and ^{16}O ($\vec{e}, e'p$) reactions over the quasielastic region at Q^2 of 0.25, 0.6, and 1.0 (GeV/c) 2 . The observable A_e is related to the "fifth structure function", which is primarily sensitive to final state interactions and therefore to the p-N optical potential. We request 480 hours of beam time for this study.

1 Introduction

1.1 Physics Motivation

The $(\vec{e}, e'p)$ cross section, corresponding to the reaction depicted in Figure 1 with polarized electrons and an unpolarized target, can be written in the one-photon exchange approximation as [Bo85, Bo92]

$$\begin{aligned} d\sigma &= d\sigma_{\text{Mott}}(\rho_{00}f_{00} + \rho_{11}f_{11} + \rho_{01}f_{01} \cos \phi_{pq} + \rho_{1-1}f_{1-1} \cos 2\phi_{pq} + h\rho'_{01}f'_{01} \sin \phi_{pq}) \\ &= \Sigma + h\Delta \end{aligned}$$

where $d\sigma_{\text{Mott}}$ is the cross section for scattering from a point charge, and ϕ_{pq} is the azimuthal reaction angle for the emitted proton as defined in Figure 1. The ρ_{ij} are elements of the lepton tensor, and the f_{ij} are the nuclear structure functions, which contain all of the information pertaining to the scatterer.

Each of the structure functions exhibits a different sensitivity to the underlying details of the microscopic nuclear theory. Single arm measurements access only the transverse f_{11} and longitudinal f_{00} structure functions. Coincident cross sections without electron or target polarization contain two additional interference structure functions, f_{1-1} and f_{01} , which can be separated by multiple measurements at values of ϕ_{pq} on a cone centered on \vec{q} . A fifth structure function, f'_{01} , can be observed if the incident electrons are longitudinally polarized and out-of-plane detection is implemented.

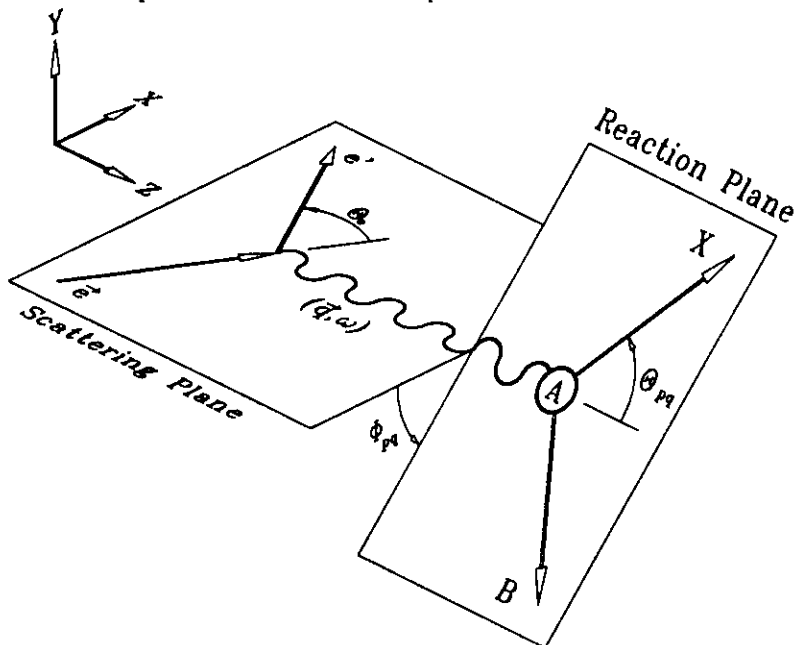


Figure 1: The fifth structure function in $A(e, e'p)B$ kinematics is in general non-zero only when the knock-out proton is detected out of the scattering plane ($\sin \phi_{pq} \neq 0$).

The helicity dependent term in the cross section, which is proportional to f'_{01} , can be isolated with small systematic error through an asymmetry measurement:

$$A_e = \frac{d\sigma_{+h} - d\sigma_{-h}}{d\sigma_{+h} + d\sigma_{-h}} = \frac{\Delta}{\Sigma}$$

Note that A_e vanishes in the electron scattering plane, where $\theta_{pq} = 0$ (parallel kinematics) or $\sin \phi_{pq} = 0$. A_e is insensitive to systematic uncertainties in the target thickness, charge collection, and all spectrometer efficiencies because these quantities cancel in the ratio. The fifth structure function can be determined from A_e and an absolute measurement of the unpolarized cross section, Σ .

$$f'_{01} = \frac{A\Sigma}{h\rho'_{01}d\sigma_{\text{Mott}}} .$$

f'_{01} arises from the interference between two or more reaction amplitudes with different phases. This constitutes a necessary condition for obtaining an imaginary component in the transverse-longitudinal interference response. In the plane wave impulse approximation [Bo85, Co87], the fifth structure function vanishes. In the case of quasi-elastic proton knock-out kinematics, measurements of this observable are primarily sensitive to the final state interactions (FSI) of the emitted proton. The interference between the dominant knock-out amplitude and the rescattering (multistep) amplitude results in a non-zero imaginary component in the transverse-longitudinal interference response.

A prediction [Bo85] of the coincidence cross sections for the $p_{1/2}$ and $p_{3/2}$ states in ^{16}O at low Q^2 versus the angle θ_{pq} above and below the electron scattering plane (or, equivalently, for opposite electron helicities) is shown in Figure 2. These asymmetries are totally The difference between the cross sections above and below the plane are entirely due to the f'_{01} term in the cross section. The solid line in the figure uses the bound state wave function of Elton and Swift (ES) and the optical potential of Jackson and Abdul-Jalil (JA), and the dashed line uses the wave function and optical potential of Giannini and Ricco (GR). The asymmetry is more pronounced for the ES-JA combination than for the GR one indicating the central role of the spin term in the final distortion.

While theoretical models have achieved a large degree of success in describing the available data for these reactions, further progress requires a better understanding of FSI. Distorted-wave impulse approximation calculations consistently overestimate the spectroscopic factors (shell occupancies) and additionally contain theoretical uncertainties of order 10% in the cross section resulting from the treatment of FSI [Be82]. FSI complicate the extraction of the spectroscopic factors and introduce significant model error to contributions from more subtle effects such as nucleon correlations [Bo91]. To further refine the microscopic nuclear theory and quantify the role of effects such as meson exchange currents (MEC) and isobar configurations (IC), FSI must first be understood.

FSI are generally modeled using phenomenological optical potentials derived from proton elastic scattering. Potentials chosen to reproduce elastic proton scattering describe

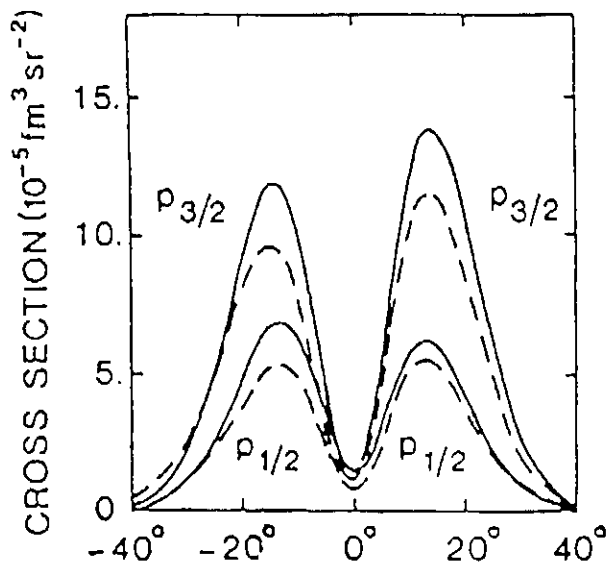


Figure 2: Coincidence cross section as a function of ϕ_{pq} for the $p_{1/2}$ and the $p_{3/2}$ hole in the $^{16}\text{O}(e,e'p)^{15}\text{N}$ reaction. [Bo85]. The solid line is ES-JA, and the dashed is GR (as defined in the text).

only the asymptotic behavior of the knock-out proton in $(e, e'p)$, while FSI are sensitive to the component of the proton wave function inside the nucleus. The fifth structure function, therefore, provides the observable of choice to test the theoretical treatment of FSI.

1.2 Measurement

We propose to inaugurate a program of out-of plane measurements at CEBAF on a number of nuclei. We propose to start this program with measurements on ^{16}O and ^{12}C . It is confirmed by our Bates experiment that the measurement of the fifth structure function is the simplest way to start such a program. We will attempt to expand this program to heavy nuclei and the isolation of the f_{1-1} interference structure function in the future depending upon our experience with this first measurement at CEBAF and the performance achieved by the out of plane facility in Hall C.

We propose to measure A_e as a function of θ_{pq} at $Q^2 = 0.25, 0.6, \text{ and } 1.0 \text{ (GeV/c)}^2$ in quasi-elastic kinematics on ^{12}C and ^{16}O . Using the out-of-plane capability of the SOS-HMS system [Do92], we will cover a range in θ_{pq} from 0° to roughly 20° at each Q^2 point.

The count rates for both targets are quite favorable at each Q^2 point. Given that angle changes of the SOS comprise a substantial fraction of our requested time, it is sensible to acquire data on both targets at each angle. A measurement of FSI through the fifth structure function, together with a separation of the first four structure functions, will severely constrain all theoretical models and enable a detailed examination of nucleon correlations. As a doubly closed shell nucleus, oxygen provides an important test of shell model calculations. The Pavia, Argon, and Illinois theoretical efforts will yield very precise calculations on this system, and for that reason, ^{16}O presents a particularly interesting case. The carbon measurements will complement the large body of existing in-plane $^{12}\text{C}(e, e'p)$ data. From an experimental viewpoint, carbon is a very convenient target. With the relatively large asymmetries and high count rates which are anticipated, we want to develop the ^{12}C fifth structure function measurement as a calibration standard for other nuclei.

We will investigate the Q^2 dependence of the fifth structure function at three points using a single beam energy of 2 GeV. The $0.25 (\text{GeV}/c)^2$ point was chosen to provide continuity with the accessible Q^2 range at the Bates Laboratory and the measurements using the Out Of Plane Spectrometers (OOPS). The $0.6 (\text{GeV}/c)^2$ measurements will complement the approved Hall A measurement [Lo89] on ^{16}O , which will use the same Q^2 and extract f_{11} , f_{01} , and a linear combination of f_{00} and f_{1-1} . The experimental kinematics allow us to extend the investigation of the Q^2 dependence of the fifth structure function to $1.0 (\text{GeV}/c)^2$ with count rates which are still quite reasonable.

2 Experimental Status

The first and only measurements of the fifth structure function occurred at Bates using the $^{12}\text{C}(\vec{e}, e'p)$ [Man93] and $^2\text{H}(\vec{e}, e'p)$ reactions in quasi-elastic kinematics. Figure 3 compares the measured carbon asymmetries and structure functions with theoretical calculations by Radici and Boffi for different optical potentials. Within each set, the inclusion of MEC and IC (Δ only) produces only small variations. All the calculations have been corrected for coulomb distortion of the incident electron [Gi76]. The curves show a strong dependence of f'_{01} on the selection of an optical potential and a relative insensitivity to other effects.

All three optical potentials employed in Figure 3 are phenomenological models with the Woods-Saxon radial shape. Each potential includes real and imaginary central terms and a real spin-orbit component; the CK and S potentials additionally include an imaginary spin-orbit contribution. The uncertainties of the two carbon points are primarily statistical.

These first fifth structure function data illustrate the potential of such measurements. The ^{12}C data were acquired in just 64 hours using a low duty factor (0.85%) machine and a modest luminosity of less than $1 \mu\text{A}\cdot\text{g}/\text{cm}^3$. Typical trues to accidentals ratios were 1/2. The low systematic error which is attainable with asymmetries is illustrated by the small error bars on the point at $\theta_{pq} = 0^\circ$. This was a systematic error check using a deuterium

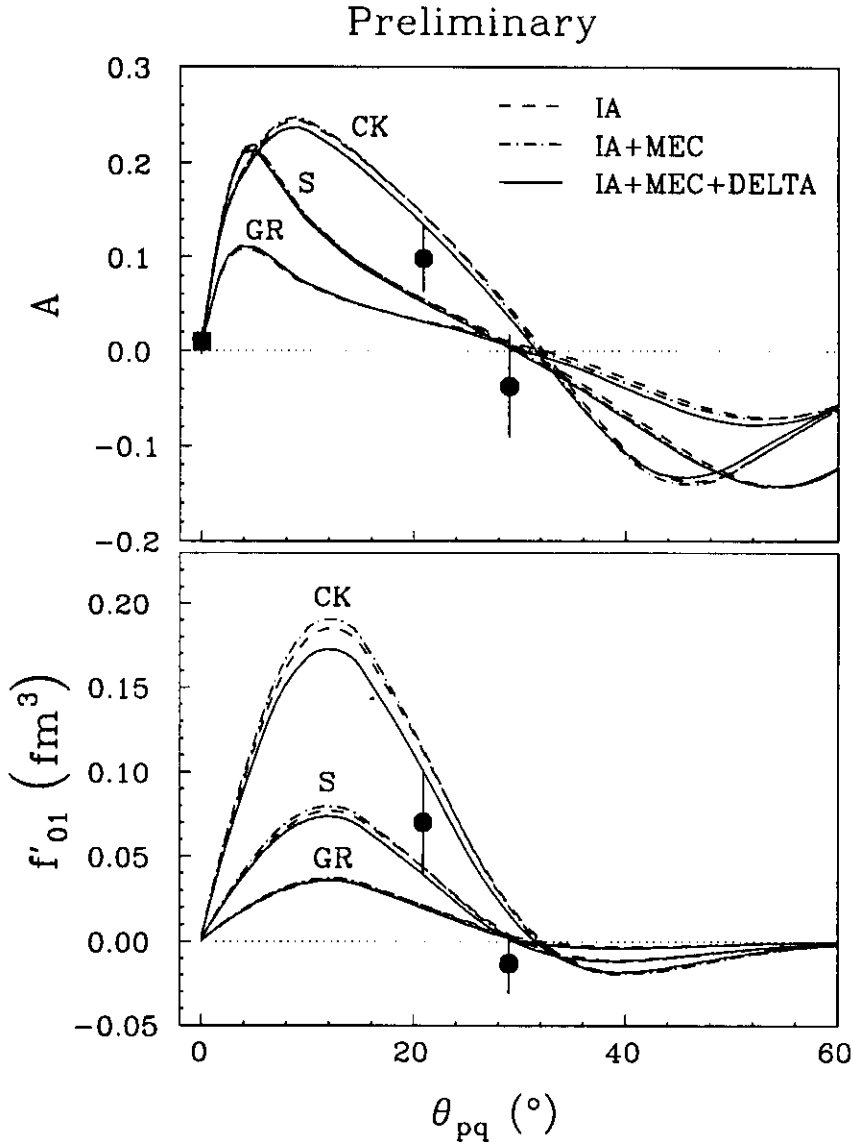


Figure 3: Preliminary results for the first fifth structure function measurement [Man93] are compared to theoretical predictions in the impulse approximation (IA) for different optical potentials with and without MEC and IC. CK denotes the optical potential of Comfort and Karp [Ck80], S is that of Schwandt et al. [Sc82], and GR is the Giannini and Ricco potential [Gi76].

target. By using higher luminosities with the high duty factor machine at CEBAF, much higher precision measurements can be attained in a matter of hours.

3 Experimental Apparatus

The impact of this experiment on laboratory facilities is modest. We will use the HMS and SOS spectrometers in configurations which are compatible with their published capabilities, and we plan no modifications to the standard focal plane instrumentation for

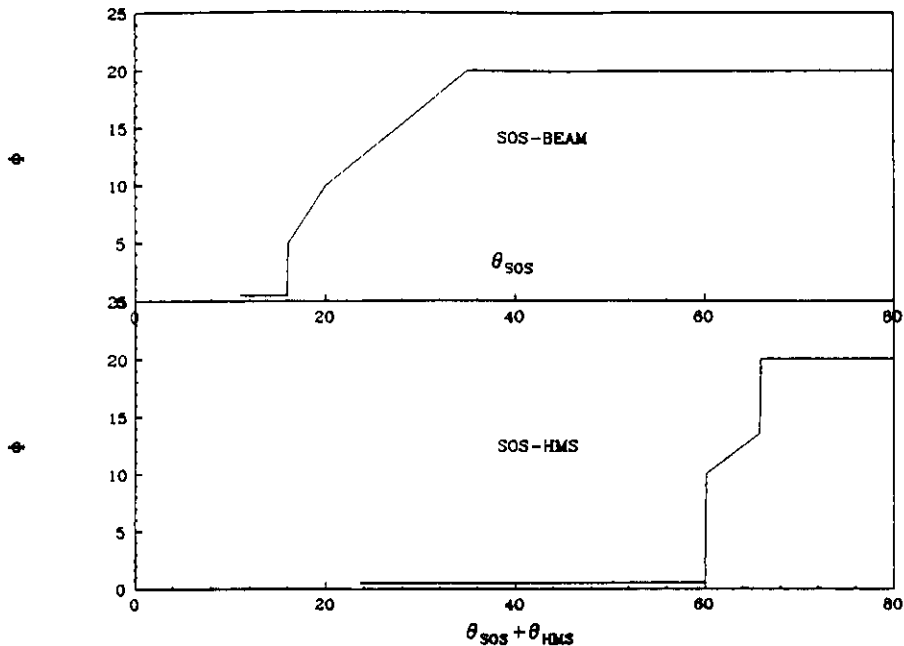


Figure 4: Limits to out-of-plane motion of the SOS as function of (Top) the angle between the SOS and the beam line, and (Bottom) the angle between the SOS and HMS.

either spectrometer. We will use a waterfall target for our ^{16}O measurements of the type planned for the approved ^{16}O measurement [Lo89] in Hall A. The polarization, stability, and current provided the electron source at CEBAF are adequate for our measurements.

3.1 Spectrometers

An enhancement to the design of the SOS has added the means to move that spectrometer out of plane [Do92]. The Hall C spectrometer pair represents the only out-of-plane capability using focusing spectrometers at CEBAF. The published resolution of the Hall C magnetic spectrometers provides adequate missing energy resolution for our measurements.

Several papers have been presented on the out-of-plane capability of the SOS and a physics program which takes advantage of this property [We92, Mac92, Wo92]. Figure 4 shows the restrictions on out-of-plane operation [Wo92]. The carriages and front quadrupoles for the HMS and SOS have been designed so that these spectrometers can be moved as close to each other and the beam line as possible. The carriages are at different elevations above the floor so that the simultaneous minimal angles with respect to the beam line of the HMS and the SOS are 12.5° and 11° , respectively. These small angles can not be attained, however, if the SOS is out of plane. At small SOS angles, an out-of-plane setting is precluded by the interference between the SOS carriage and the beam line. To

	$\delta p/p$	$\Delta p/p$	$\delta\theta$ (mr)	$\delta\phi$ (mr)	$\Delta\Omega$ (msr)
HMS	10^{-3}	10%	2	2	6.4
SOS	10^{-3}	40%	2	2	9.0

Table 1: Resolutions and apertures of the HMS and SOS for point-to-point tunes in X and Y.

allow the maximum out-of-plane capability of 20° , which we desire for this experiment, the SOS is restricted to angles in the scattering plane larger than 36° . Furthermore, to avoid obstructions between the out-of-plane SOS and the first quadrupole of the HMS, a relative spectrometer angle of at least 66° must be maintained. Our kinematics, which are listed in Table 2, satisfy all these constraints.

For the proposed range of Q^2 , electrons will be detected in the HMS and protons in the SOS. Spectrometer tunes which are point-to-point in the transversion direction will be used in order to maximize the angular acceptances. The resulting momentum resolutions for the two spectrometers will conservatively be 10^{-3} . Table 1 summarizes the apertures and momentum resolutions for this tune. The configuration of the HMS and SOS detector packages will be the standard ones found in the CDR (Figure 5) [Cd90].

3.2 Target

We plan to use ^{12}C target thicknesses of 100, 200, and 300 mg/cm^2 . The 100 mg/cm^2 target minimizes proton energy loss in the target for the 135 MeV protons at our lowest Q^2 . The thicker targets were chosen to increase counting rates at the higher Q^2 points while maintaining a missing energy resolution of approximately 2 MeV. The selection of carbon targets is somewhat flexible and will be based upon the number of targets which is compatible with the water fall target for the ^{16}O measurements.

The ^{16}O target requirement can be met with a vertically oriented flowing water target [Vo91]. This target is also required for an approved Hall A measurement [Lo89]. Our desired luminosity combines a target thickness of 300 mg/cm^2 with 30 μA beam intensity. The target cylinder will be 0.3 cm diameter and have 2 micron ($1.6 \text{ mg}/\text{cm}^2$) thick Havar walls. The total wall thickness will be less than 2% of the target thickness. The tensile stress on the walls will be 15,000 psi; Havar has a yield strength of 300,000 psi. Target thickness fluctuations divide out of an asymmetry measurement. To extract the fifth structure function with a normalized absolute measurement, the beam position must be adequately monitored, since the thickness of a cylinder is position dependent. A position stability of 300 microns will limit target length fluctuations to less than 1%.

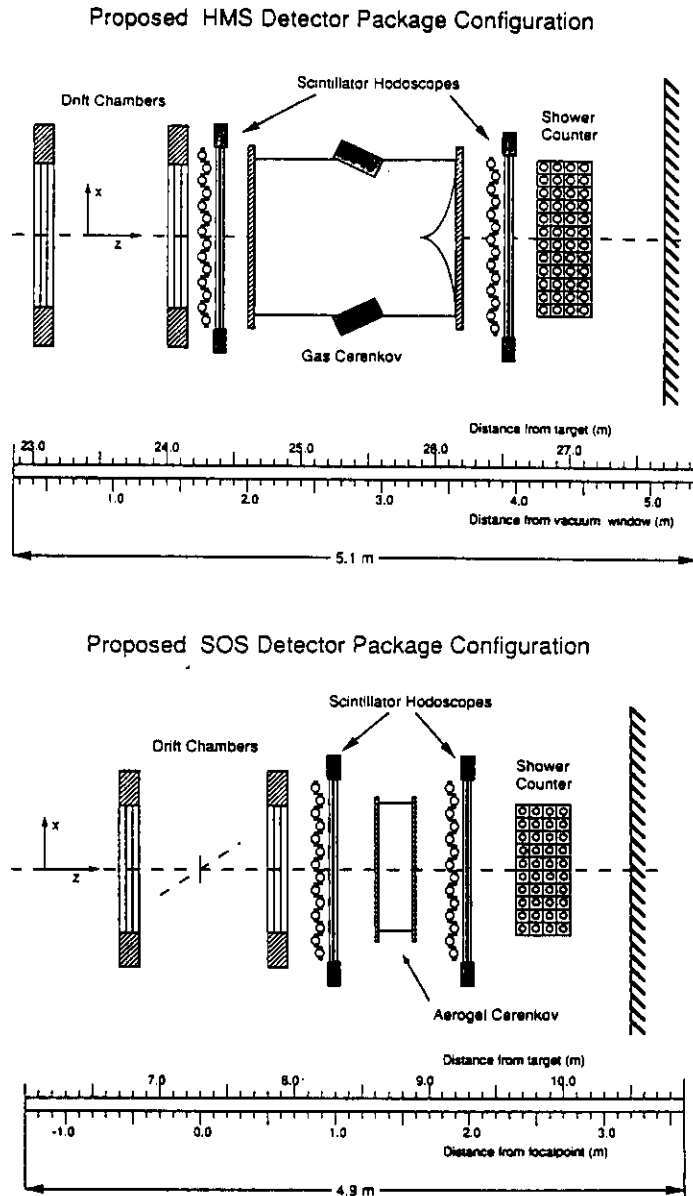


Figure 5: Schematic diagram of the standard HMS and SOS detector packages, which satisfy the requirements of this experiment.

3.3 Polarized Beam

The polarized electron source to be used in experiments at CEBAF is under development by a group led by Larry Cardman [Car93]. The source is expected to be able to deliver up to $200 \mu\text{A}$ with a polarization of 0.49. Stabilities of the current and polarization over helicity flips are expected to be better than 10^{-5} and thus exceed our requirements by several orders of magnitude. We estimate polarized source down time to be no more than 1 hour in 24 hours.

Q^2 (GeV/c) ²	θ_e (deg)	θ_q (deg)	ω (MeV)	q (MeV/c)
0.25	15.0	67.6	135.4	522.3
0.62	25.0	55.2	332.9	833.5
1.04	35.0	45.4	556.5	1142.0

Table 2: Our proposed quasi-elastic kinematics for a 2 GeV beam energy.

The beam polarization will be monitored with a Møller polarimeter. We assume that this will be a fully supported feature of Hall C. A conservative estimate of the measurement error of the polarization is $\pm 5\%$. The highest precision used for our count rate estimates does not exceed about 5% in the quantity $\delta A_e/A_e$, where we have used projections of A_e from our Pavia collaborators.

4 Kinematics

We plan to map the fifth structure function in quasi-elastic kinematics versus the angle θ_{pq} between the momentum transfer vector and the knock-out proton at an azimuthal angle of $\phi_{pq}=90^\circ$. A_e must vanish in parallel kinematics ($\theta_{pq}=0^\circ$), and this will provide a systematic error check. Table 2 shows our electron kinematics and the angle of the proton spectrometer in the scattering plane.

Identification of the final state is through the missing energy, which is defined as the energy transfer minus the final state kinetic energies. This, then, is just the proton binding energy plus the excitation of the residual nucleus.

$$E_m = E_e - E'_e - T_p - T_r$$

where E_e is the beam energy, E'_e is the energy of the scattered electron, T_p is the proton kinetic energy, and T_r is the kinetic energy of the recoil daughter nucleus. The largest contributions to the missing energy resolution are the intrinsic spectrometer momentum resolutions and the energy loss of protons in the target. The spectrometers together define a missing energy resolution of slightly better than 2 MeV. The energy loss of protons in the target is largest at the smallest Q^2 point, and for a given target thickness, this effect is relatively more important in the carbon target than the waterfall target for geometrical reasons. With our selection of target thicknesses, we have limited the proton energy loss in the target to less than 2 MeV, and thus we expect a missing energy resolution of this order.

5 Count Rate Estimates

The coincidence cross sections have been calculated using a program of Boffi, Giusti, and Pacati which has been slightly modified to work at higher energies. The single arm electron

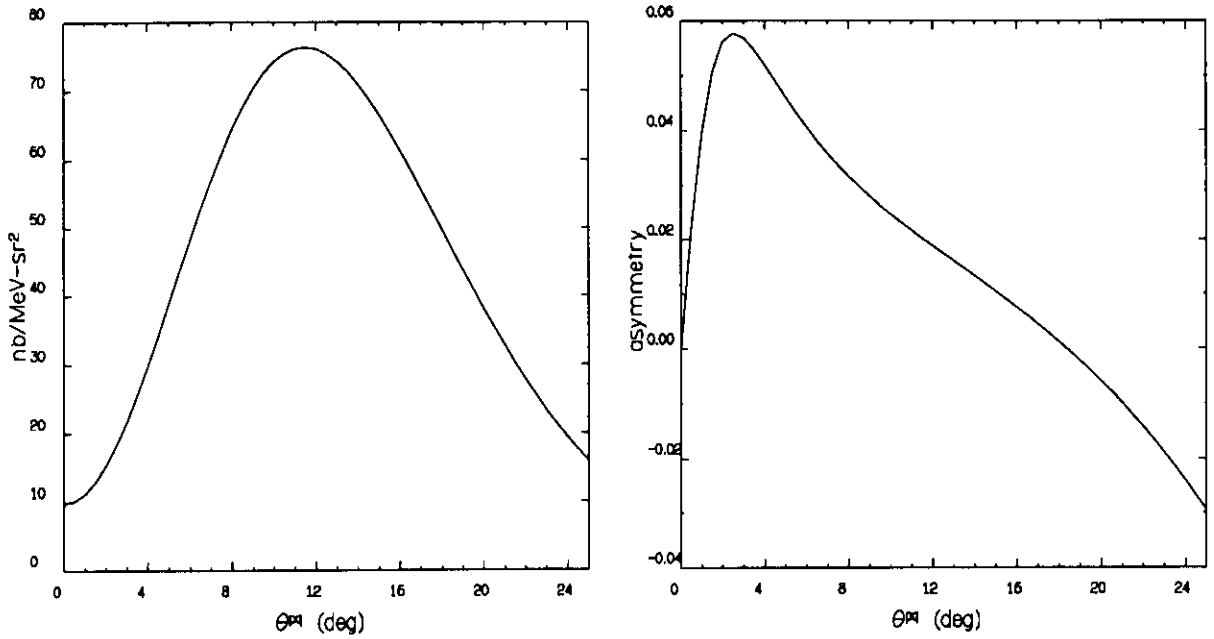


Figure 6: The carbon cross section and asymmetry used for count rate calculations are plotted versus θ_{pq} at $Q^2 = 0.25 \text{ GeV}^2$.

Polarization =	40%	Duty Factor =	100.0%
Target Thickness =	100.0–300.0 mg/cm ²	Window Thickness =	1.6 mg/cm ²
$\Omega_e =$	6.4 msr	$\Delta P_e =$	5%–10%
$\Omega_p =$	9.0 msr	$\Delta P_p =$	40%
Coincidence Window =	2 ns	Beam current =	30 μA

Table 3: Count rate parameters.

and proton counting rates are calculated using the cross section codes from Lightbody and O'Connell [Li88]. Figure 6 shows a sample cross section and asymmetry calculation for carbon at the lowest Q^2 point.

Table 3 shows our count rate parameters. The solid angles are 6.4 msr for the electron spectrometer (HMS) and 9.0 msr for the the proton spectrometer (SOS). A 40 % polarized beam with a duty factor of 100% is assumed.

Since we are measuring discrete state excitations, the kinematics are over-determined. For the calculation of the trues rate, the electron momentum bite is the minimum of the actual spectrometer bite and the kinematically determined matching bite. The three bites used in count rate calculations for the true coincidence rate were determined from a Monte Carlo simulation for $^{12}\text{C}(e, e'p)$ and are 5%, 10%, and 10% at Q^2 equal to 0.25, 0.60, and 1.0 $(\text{GeV}/c)^2$, respectively. For the calculation of accidentals, we can simulate the efficiency of a missing energy cut by using the proton momentum bite which corresponds to our

θ_{pq} (deg)	^{12}C $p_{3/2}$ (Hrs)	^{12}C $p_{3/2}$ (T/A)	^{16}O $p_{1/2}$ (Hrs)	^{16}O $p_{1/2}$ (T/A)
0	0.8	1.1	1.1	2
2	0.5	2.9	0.4	5
4	0.3	6.0	0.3	11
8	0.1	13.2	0.2	20
12	0.1	15.9	0.2	15
16	0.2	25.3	0.4	7
20	0.2	15.5	1.2	2
Total Hrs.	$2.2 \times 2 = 4.4$		$3.8 \times 2 = 7.6$	
Angle Change	30.0			
Møller, Calibration	6.0			
Contingency	10.0			
Total Hrs;	58.0			

Table 4: Fifth structure function run scenario for $Q^2 = 0.25$ (GeV/c)² points. Time is chosen to obtain δA_e of $\pm 0.2\%$.

missing energy resolution via the transformation $\delta p = \delta E_m / \beta_p$. The proton arm resolution for accidental coincidence rejection is less than 1% in all cases.

Three different thickness of ^{12}C targets have been used in these rate estimates. For the $Q^2 = 0.25$ (GeV/c)² run, the target thickness will be reduced to 100 mg/cm² to minimize proton energy loss in the target and to increase the signal to noise ratio. As energy loss becomes less important at higher proton momenta, we used thicker targets of 200 and 300 mg/cm² at .6 and 1.0 (GeV/c)², respectively.

We assume a beam current of 30 μA except at the lowest Q^2 for ^{16}O , where the current is reduced to 10 μA to obtain a reasonable signal to noise ratio.

6 Beam Request

The estimated running time for both ^{12}C and ^{16}O are tabulated in the Tables 4, 5, and 6. The total estimated beam time to execute the proposed experiment is 480 hours. The hours given in these tables are required beam time to obtain an error in the experimental asymmetry of 0.2 % for $Q^2 = 0.25$ and 0.6 (GeV/c)². An asymmetry error of 0.5 % will be obtained at $Q^2 = 1.0$ (GeV/c)². We have multiplied the beam hours by two to subdivide the electron spectrometer momentum bite. The time required for angle changes is not insubstantial. Six hours are required to change the out-of-plane angle from 0 to 20 °, and somewhat less time is needed for smaller angle changes.

θ_{pq} (deg)	^{12}C $p_{3/2}$ (Hrs)	^{12}C $p_{3/2}$ (T/A)	^{16}O $p_{1/2}$ (Hrs)	^{16}O $p_{1/2}$ (T/A)
0	3.9	86		8
2	1.3	77	3.0	32
4	0.5	193	1.2	80
8	0.4	250	0.9	120
12	0.7	161	1.8	57
16	2.3	48	6.9	15
20	12.9	8	38.8	2
Total Hrs.	22.0 x 2 = 44.0		52.6 x 2 = 105.2	
Angle Change	30.0			
Møller, Calibration	30.0			
Contingency	30.0			
Total Hrs;	239.2			

Table 5: Fifth structure function run scenario for $Q^2 = 0.6$ (GeV/c)² points. Time is chosen to obtain δA_e of $\pm 0.2\%$.

θ_{pq} (deg)	^{12}C $p_{3/2}$ (Hrs)	^{12}C $p_{3/2}$ (T/A)	^{16}O $p_{1/2}$ (Hrs)	^{16}O $p_{1/2}$ (T/A)
0	6.8	61		
2	0.6	733	1.2	483
4	0.3	1890	0.5	980
8	0.3	1455	0.8	494
12	1.3	354	3.8	376
16	11.8	39	30.2	3
Total Hrs.	21.1 x 2 = 42.2		35.5 x 2 = 71.0	
Angle Change	30.0			
Møller, Calibration	20.0			
Contingency	20.0			
Total Hrs;	183.2			

Table 6: Fifth structure function run scenario for $Q^2 = 1.0$ (GeV/c)² points. Time is chosen to obtain δA_e of $\pm 0.5\%$.

7 Summary

The high energy, high duty factor accelerator at CEBAF will increase the precision of electron scattering coincidence measurements. Under these new circumstances, measurements can become more exclusive. In particular, the fifth structure function can be measured in a variety of reactions using the out of plane capability of the SOS spectrometer. A large body of $(e, e'p)$ data exists on a variety of nuclei, yet the interpretation of this data within microscopic models is hampered by the theoretical ambiguity in the role of final state interactions. The fifth structure function asymmetry is a consequence of FSI and can be measured with small systematic error. The size of the asymmetries are relatively large.

(5–10%) and the count rates are reasonable. We propose measurements at three different Q^2 on ^{16}O and ^{12}C . We request 480 hours of beam time for this study.

References

- [Be82] M. Bernheim et al., Nucl. Phys. **A375**, 381 (1982).
- [Bo85] S. Boffi, C. Giusti, and F. D. Pacati, Nucl. Phys. **A435**, 697 (1985).
- [Bo91] S. Boffi and M. Radici, Nucl. Phys. **A526**, 602 (1991).
- [Bo92] S. Boffi, C. Giusti, and F. D. Pacati, Phys. Rep. (1992).
- [Car93] L. S. Cardman, private communication.
- [Cd90] CEBAF Conceptual Design Report, (1990).
- [Ck80] J. R. Comfort and B. C. Karp, Phys. Rev. C **21**, 2162 (1980).
- [Co87] G. Co, M. Lallena, and T. W. Donnelly, Nucl. Phys. **A469**, 684 (1987).
- [Da93] D. Day and N. Phillips, “Cerenkov Detector Design”, unpublished.
- [Do92] J. D. Domingo, R. D. Carlini, B. A. Mecking, and J. Y. Mougey, CEBAF 1992 Summer Workshop, AIP Conference Proceedings, **269**, 25 (1992).
- [Gi87] C. Giusti and F. D. Pacati, Nucl. Phys. **A473** (1987) 717; Nucl. Phys. **A485**, 461 (1988).
- [Gi76] M. M. Giannini and G. Ricco, Ann. of Phys. **102**, 458 (1976).
- [Lo89] R. W. Lourie, et al., CEBAF proposal 89-03 (1989).
- [Mac92] D. J. Mack, CEBAF 1992 Summer Workshop, AIP Conference Proceedings, **269** 468 (1992).
- [Man93] J. B. Mandeville, et al., to be published.
- [Li88] J. W. Lightbody Jr. and J. S. O’Connell, Comp. in Phys. May-June **57** (1988).
- [Sc82] P. Schwandt, H. O. Meyer, W. W. Jacobs, A. D. Bacher, S. E. Vigdor, M. D. Kaitchuck, and T. R. Donoghue, Phys. Rev. C **26**, 55 (1982).
- [Vo91] N. Voegler, J. Friedrich, E. A. J. M. Offerman, C. W. de Jager, and H. de Vries, Phys. Rev. C **43**, 2172 (1991).
- [We92] L. B. Weinstein, CEBAF Summer Workshop, AIP Conference Proceeding, **269**, 438 (1992).
- [Wo92] S. A. Wood, CEBAF Summer Workshop, AIP Conference Proceeding, **269**, 560 (1992).